ARL-RP-0549 ● SEP 2015

US Army Research Laboratory

High Resolution Numerical Simulations of Primary Atomization in Diesel Sprays with Single Component Reference Fuels

by L Bravo, D Kim, M Tess, M Kurman, F Ham, and C Kweon

Reprinted from ILASS-Americas. Paper presented at the 27th Annual Conference on Liquid Atomization and Spray Systems; 2015 May; Raleigh, NC.

NOTICES

Disclaimers

The findings in this report are not to be construed as an official Department of the Army position unless so designated by other authorized documents.

Citation of manufacturer's or trade names does not constitute an official endorsement or approval of the use thereof.

Destroy this report when it is no longer needed. Do not return it to the originator.

ARL-RP-0549 ● SEP 2015

US Army Research Laboratory

High Resolution Numerical Simulations of Primary Atomization in Diesel Sprays with Single Component Reference Fuels

by L Bravo, M Tess, M Kurman, and C Kweon
Vehicle Technology Directorate, ARL

D Kim and F Ham
Cascade Technologies Inc, Palo Alto, CA

Reprinted from ILASS-Americas. Paper presented at 27th Annual Conference on Liquid Atomization and Spray Systems; 2015 May; Raleigh, NC.

REPORT DOCUMENTATION PAGE

Form Approved
OMB No. 0704-0188

1. REPORT DATE *(DD-MM-YYYY)*	2. REPORT TYPE	3. DATES COVERED (From - To)
September 2015	Reprint	January–September 2014

4. TITLE AND SUBTITLE
High Resolution Numerical Simulations of Primary Atomization in Diesel Sprays with Single Component Reference Fuels

5a. CONTRACT NUMBER

5b. GRANT NUMBER

5c. PROGRAM ELEMENT NUMBER

6. AUTHOR(S)
L Bravo, D Kim, M Tess, M Kurman, F Ham, and C Kweon

5d. PROJECT NUMBER

5e. TASK NUMBER

5f. WORK UNIT NUMBER

7. PERFORMING ORGANIZATION NAME(S) AND ADDRESS(ES)
US Army Research Laboratory
ATTN: RDRL-VTP
Aberdeen Proving Ground, MD 21005-5066

8. PERFORMING ORGANIZATION REPORT NUMBER
ARL-RP-0549

9. SPONSORING/MONITORING AGENCY NAME(S) AND ADDRESS(ES)

10. SPONSOR/MONITOR'S ACRONYM(S)

11. SPONSOR/MONITOR'S REPORT NUMBER(S)

12. DISTRIBUTION/AVAILABILITY STATEMENT
Approved for public release; distribution is unlimited.

13. SUPPLEMENTARY NOTES
Reprinted from ILASS-Americas. Paper presented at 27th Annual Conference on Liquid Atomization and Spray Systems; 2015 May; Raleigh, NC.

14. ABSTRACT

A high-resolution numerical simulation of jet breakup and spray formation from a complex diesel fuel injector at diesel engine type conditions has been performed. A full understanding of the primary atomization process in diesel fuel injection has not been achieved for several reasons including the difficulties accessing the optically dense region. Due to the recent advances in numerical methods and computing resources, high resolution simulations of atomizing flows are becoming available to provide new insights of the process. In the present study, an unstructured un-split Volume-of-Fluid (VoF) method is employed to simulate the injection event with prescribed bulk inflow conditions. An axial single-hole ARL fuel injector was X-ray scanned at The Advanced Photon Source Facility from Argonne National Laboratory for this work to define the internal geometry. The working conditions correspond to orifice dimensions of 90μm fueled with n-paraffin (n-dodecane) and iso-paraffin (iso-octane) reference fuels for a detailed investigation of fuel specific mixing mechanisms. The spray releases into a quiescent chamber filled with 100% Nitrogen at ambient conditions at 20 *bar*, 300*K* with $6.9x10^4 < Re < 2.5x10^4$ and $5.4x10^4 < We < 1.25x10^5$ both with $Oh > Oh_{cr}$ setting the spray in the full atomization mode. The simulations provide detailed diagnostics in the optically dense region extending from $5 < x/d < 25$ jet diameters. The results provide insights on the effect of start-of-injection on the velocity and volume fraction fields for each fuel at a range of pressures. High resolution backlit imaged data in the near nozzle region recently acquired at the Army Research Laboratory are used to provide validation metrics for the spray breakup length and dispersion characteristics.

15. SUBJECT TERMS
multiphase flows, spray, turbulence

16. SECURITY CLASSIFICATION OF:			17. LIMITATION OF ABSTRACT	18. NUMBER OF PAGES	19a. NAME OF RESPONSIBLE PERSON
a. REPORT	b. ABSTRACT	c. THIS PAGE			L Bravo
Unclassified	Unclassified	Unclassified	UU	16	19b. TELEPHONE NUMBER (Include area code) 410-278-9525

ILASS-Americas 27th Annual Conference on Liquid Atomization and Spray Systems, Rayleigh, NC, May 2015

High Resolution Numerical Simulations of Primary Atomization in Diesel Sprays with Single Component Reference Fuels

L. Bravo[*1], D. Kim[2], M. Tess[1], M. Kurman[1], F. Ham[2] and C. Kweon[1]
[1]U.S. Army Research Laboratory, APG, MD 21005
[2]Cascade Technologies Inc, Palo Alto, CA, 94303

A high-resolution numerical simulation of jet breakup and spray formation from a complex diesel fuel injector at diesel engine type conditions has been performed. A full understanding of the primary atomization process in diesel fuel injection has not been achieved for several reasons including the difficulties accessing the optically dense region. Due to the recent advances in numerical methods and computing resources, high resolution simulations of atomizing flows are becoming available to provide new insights of the process. In the present study, an unstructured un-split Volume-of-Fluid (VoF) method is employed to simulate the injection event with prescribed bulk inflow conditions. An axial single-hole ARL fuel injector was X-ray scanned at The Advanced Photon Source Facility from Argonne National Laboratory for this work to define the internal geometry. The working conditions correspond to orifice dimensions of 90μm fueled with n-paraffin (n-dodecane) and iso-paraffin (iso-octane) reference fuels for a detailed investigation of fuel specific mixing mechanisms. The spray releases into a quiescent chamber filled with 100% Nitrogen at ambient conditions at 20 *bar*, 300*K* with $6.9x10^4 < Re < 2.5x10^4$ and $5.4x10^4 < We < 1.25x10^5$ both with $Oh > Oh_{cr}$ setting the spray in the full atomization mode. The simulations provide detailed diagnostics in the optically dense region extending from $5 < x/d < 25$ jet diameters. The results provide insights on the effect of start-of-injection on the velocity and volume fraction fields for each fuel at a range of pressures. High resolution backlit imaged data in the near nozzle region recently acquired at the Army Research Laboratory are used to provide validation metrics for the spray breakup length and dispersion characteristics.

[*]Corresponding author: luis.g.bravo2.civ@mail.mil

Introduction

Multiphase flows are of significant interest to the engineering and military community as they play an important role in several ground/aerial propulsion and power generation applications. They are also relevant in a broader scientific context in applications ranging from aerosol dynamics, fire suppression, and coating applications to name a few. For most of these applications, an accurate description of the interface location is generally difficult to achieve as resolution can be limited. In particular for diesel liquid sprays the complexity is further compounded by the physical attributes present including nozzle turbulence, large density ratios, complex evaporation, the ligament/droplet formation mechanism and dispersed flow transport all in a single injection event. The spatio-temporal fluid scales needed for a complete description are also very challenging and related to the instability length scales (~1μm) and speed of the ensuing jet (~100m/s). The multiscale nature of the problem requires a high fidelity approach able to capture and describe the multiphase dynamics. Of key interest here is the need to better understand the liquid jet breakup process through a Direct Numerical Simulation (DNS) investigation aiming to resolve all relevant gas phase flow scales. The intent of DNS approach is to present a comprehensive assessment of a concurrent experimental measurement [1] and ultimately provide more accurate atomization subgrid models for engineering level descriptions. A better understanding of the underlying physics will also drive the development of next generation engines featuring higher power densities and fuel economy improving the efficiency of Army platforms and ensuring military power projection superiority.

With the continued progress in computing technology and numerical algorithms the use of highly resolved simulations to study two phase atomizing flows has become a viable alternative complementing experiments. Early pioneering works have focused on developing implicit interface capturing methods such as the volume of fluid (VoF) [2] and level set [3] and both have attracted significant attention to simulate interfacial flows involving extensive topology changes. In a recent effort [4], complex geometries found in realistic gas turbine combustor injectors have been simulated using the immersed boundary approach. The findings show good experimental agreement of the air-assisted breakup of planar and co-axial liquid layers demonstrating the efficacy of the first principles approach. Similarly in related works [5] simulations of a realistic aerospace combustor featuring multi-nozzle swirler injector were carried out providing compelling results and insights of the primary breakup physics. In diesel spray applications, several studies aiming to demonstrate the performance of numerical schemes [6-10] have been presented. Although canonical, the investigations presented a thorough analysis of the hydrodynamic instabilities, ligament formation, transport, and droplet statistics. Similar works [11] have presented the impact of density ratio and injector geometry on the atomization physics predicting the influence of the *k-factor* on the droplet number count and jet spread. As a results, subsequent efforts have focused on application of the numerical schemes to realistic injectors using a coupled nozzle flow and spray DNS approach [12]. The study correctly captured the spray parameters and dispersion characteristics when compared to experimental images carried at similar conditions. The effort also presented a database containing droplet histograms for future comparison with laboratory characterization.

Also of interest are the recent efforts targeting at developing more accurate subgrid scale models. In atomizing flows, the need to correctly identify the spray liquid structures has lead to recent algorithmic developments [13] using a tagging strategy. The method joins linear segments defining the interface and discriminates between bubbles, ligaments, droplets or sheets. The capability was tested and demonstrated in a hydraulic jump application (wave breaking region) by computing interfacial statistics yielding compelling results. More fundamental work was carried out [14-15] to study the interaction of decaying homogenous isotropic turbulence (HIT) with an interface under tension. They reported on the scales of interfacial corrugations recognizing the role of the Kolmogorov critical radius (or Hinze scale) over wide range of conditions. The importance of backscatter energy arising from the surface tension force was recognized motivating the emerging efforts in subgrid scale large-eddy simulation models [16].

The proposed body of work aims to demonstrate the capability of a recently adopted high fidelity two phase flow solver in the context of diesel engine sprays. Previous works relating to this approach demonstrate the capability of the simulation software [17-18] in accurately capturing two phase flow physics in different configurations. The applications of interest here-in are related to high speed fuel injection of single-component fuels, namely n-dodecane and iso-octane at engine like conditions. More thorough description of the working conditions is described in the following sections. The objective of the study is to provide an extensive database for engineering sub-model development and to formulate sub-grid atomization models specific for diesel high pressure fuel injection. In the next section, we will present the computational framework and methodology that was adopted in this study.

Computational Framework

The computational framework adopted in this study used a novel geometric unsplit VoF method that is conservative on unstructured meshes [17-18]. The geometric VoF method ensures discrete conservation and boundedness of the volume fraction utilizing non-overlapping flux polyhedral for donor volumes. The unstructured VoF scheme is based on the transport of the advection equation as follows,

$$\frac{\partial \rho}{\partial t} + \frac{\partial \rho u_j}{\partial x_j} = 0$$

where ρ is the mass density field and u_j is the velocity vector. Assuming each phase has constant properties the density and viscosity can be defined as a function of the advection scalar .

$$\rho = \psi\rho_1 + (1-\psi)\rho_2$$

$$\mu = \psi\mu_1 + (1-\psi)\mu_2$$

where the subscripts refer to the physical properties of fluid 1 and 2.

The VoF methodology uses a piecewise linear interface calculation (PLIC) scheme [19-20] to describe the interface requiring an interface normal, $\boldsymbol{n}$. In this scheme, the plane is located geometrically within a dual volume and oriented in the direction of the local surface normal. The surface normal is then calculated based on an upwinded advection of the previous signed distance field *(G)* to the interface. The interface vector $\boldsymbol{n}$ and the interface curvature $\boldsymbol{k}$ is calculated as follows,

$$\boldsymbol{n} = \frac{\nabla G}{|\nabla G|}$$

$$k = \nabla \cdot \boldsymbol{n}$$

The curvature is numerically discretized and the location of the plane is determined from the signed minimum distance *G* and the normal vector $\boldsymbol{n}$ from the node through a bisection algorithm. On updates of the VoF scalar, the mass flux is computed from the VoF advection and utilized in the momentum equation resulting in mass conserving, un-split, monotonic, unstructured VoF scheme. Multiple frozen velocity advection updates are performed for each momentum step to help diminish the strict over flow time step requirement of VoF schemes.

The gas phase flow solver uses a fractional step method to advance the momentum equations imposing the divergence free condition. This results in a variable coefficient Poisson system that is presently solved using a multi-grid preconditioned GMRES solver. The accuracy of the coupled two phase flow solver has been demonstrated in various canonical verification test cases including the two dimensional Zalesak disk, three dimensional sphere in deformation field, and a stationary column in equilibrium presenting accurate simulation results in an unstructured state-of-the-art framework. In addition, several successful validation studies have been performed demonstrating the applicability of the first principles approach to complex flows of interest [17-18].

Experiments for Comparison

Validation efforts are conducted through comparison with measurements carried out with our in-house database at ARL-VTD, Spray and Combustion Research Laboratory (SCRL). This is a state-of-the-art facility housing a Constant Pressure Flow (CPF) high-temperature high-pressure vessel able to provide diesel engine thermodynamic conditions. Unlike Constant Volume Preburn (CVP) vessels this rig does not require a pre-burn phase to obtain this condition and rather it is comprised of four subsystems including: gas compressor, gas heater, test vessel, and control system to achieve nearly quiescent and steady thermodynamic conditions. The facility can operate with various types of fuel injection systems. However, for the validation experiments mentioned in this work, the facility utilized a common rail fuel injection system with a Bosch CRIN3 fuel injector

Table1. Conditions for non-evaporating single-hole spray measurements and simulations.

Ambient gas temperature	303 (K)
Ambien gas pressure	20 bar
Ambient gas density	22.8 (kg/m^3)
Ambient gas N_2	100%
Nozzle K factor (nominal)	1.5
Nozzle outlet diameter (nominal)	90 um
Number of holes	1 axial
Nozzle type	sac
Aspect ratio (*l*/*d*)	7.4
Fuels (cases 1,2)	ndodecane, isooctane
Fuel injection pressure	95, 150 bar

For this work the spray transient behavior was captured by imaging the flow region near the injector tip. The injection events were imaged with a Shimadzu HPV-X frame transfer CMOS camera and a Navitar long-working distance microscope 12× zoom lens [1]. The camera was capable of recording a maximum of 256 full-frame images (400 × 250 pixels) at speeds up to 10 million frames per second with a 50 ns exposure.

More details on the optical techniques can be found on [1].

Computational Setup

An axial single-hole ARL fuel injector was X-ray scanned at The Advanced Photon Source Facility from Argonne National Laboratory for this work. Figure 1a below shows the line of sight in-situ measurement used for characterization, the image shows the axial nozzle region selection Note the adjacent orifices are not selected because they were welded shut in our injector. Figure 1b shows the rendered image used in the simulation with a description of the fuel passage ways, needle valve in the fully open position, sac volume, and nozzle passage way.

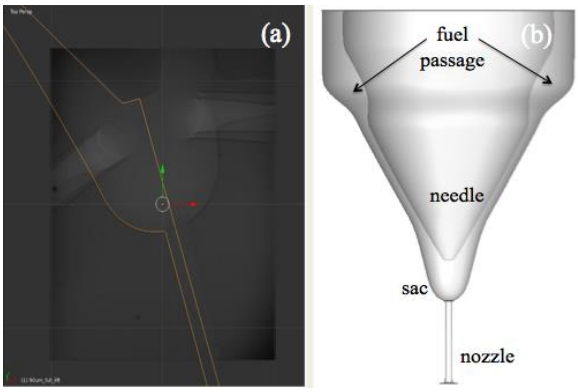

Figure1. Single-hole axial BOSCH CRIN3 injector. (a) Line of sight X-ray measurement characterization, (b) Schematic and rendered image of geometry.

In this study the working conditions correspond to nominal orifice dimensions of 90μm fueled with n-paraffin (n-dodecane) and iso-paraffin (iso-octane) reference fuels at two injection pressures of 95 bar and 150 bar with constant back pressure of 20 bar and ambient temperature of 303K as was indicated in Table1. Hence there are a total number of four cases studied in this work where the aim is to capture the full injection event from the start of injection. The physical conditions were prescribed based on an estimated fuel temperature at 298K as this was an approximation to the water-cooled jacket temperature in the experiments. Reported properties for n-dodecane [21] are as follows, density $\rho = 744\ kg/m^3$, viscosity $\mu = 1.36 mPa \cdot s$, and surface tension $\sigma = 24.7\ mN/m$. The isooctane properties reported [22] are density $\rho = 686\ kg/m^3$, viscosity $\mu = 0.478 mPa \cdot s$, and surface tension $\sigma = 18.6\ mN/m$. The chamber density was specified for nitrogen at 303K as $\rho = 22.8\ kg/m^3$. Note the simulation was initialized with the nozzle filled with liquid, this enabled the specification of rate-of-injection (ROI) mass flow rates as a bulk flow boundary condition. In addition a turbulent inflow generation condition was utilized in an effort to help transition and capture the nozzle flow turbulence.

To simulate the fuel rate-of-injection the CMT virtual injection generator was utilized. The generator is a generic hydraulic model that allows specification of orifice diameter, fuel density, injection temperature, and ambient conditions to provide accurate ROI profiles. It is provided here for reference, http://www.cmt.upv.es/ECN03.aspx.

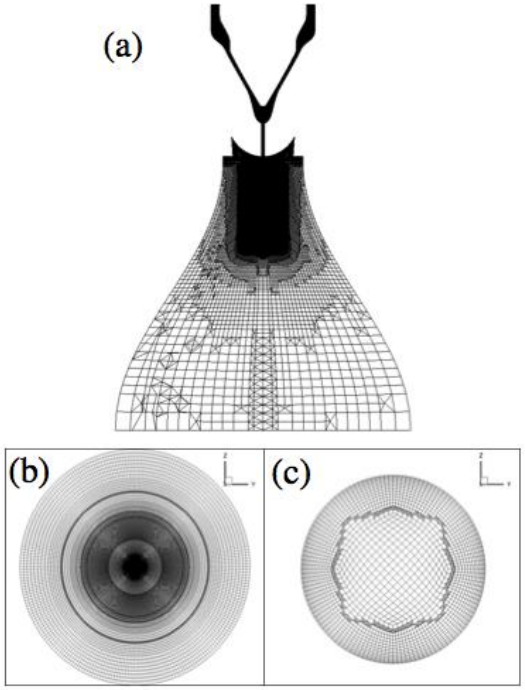

Figure 2. Computational geometry with hexahedral mesh. (a) Grid distribution along fuel passageway, nozzle, and spray chamber. Grids at (b) x/d = 5 cross sectional plane and (c) inside the nozzle.

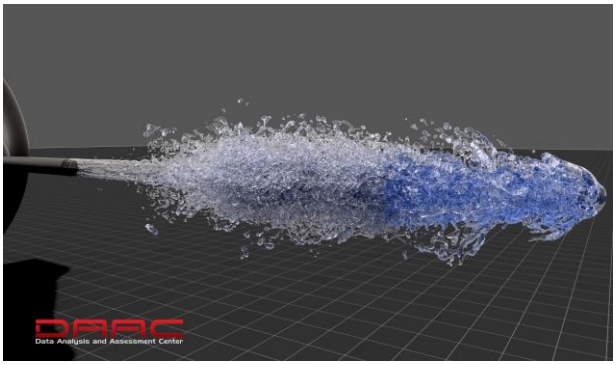

Figure 3. Structure of the diesel spray in the near nozzle region from simulations.

Figure 2a above shows the grid distribution including the injector nozzle geometry and the chamber region. Note the grid density is higher inside the nozzle region to help resolve the flow scales up to $y^+ \sim 1$. In the streamwise and spanwise directions the resolution was defined as $\Delta x^+ \sim 50$ and $\Delta z^+ \sim 20$ as these are the recommended criteria for a wall-resolved pipe flow calculation with total cell size of 77 Million grid points. A dynamic Smagorinsky large eddy simulation approach was adopted to treat the smallest flow structures and for computational efficiency in this work. In the near nozzle chamber region as shown in Figure 2b at a cross section *x/d*=5 the distribution is fine near the centerline. In the farstream and outflow, the grid is coarsened to mitigate instabilities and pressure waves flowing back upstream. Figure 3 shows the developing spray structure during the first stages of the injection event. Note the finer grid distribution captures the spray atomization region.

Results and Discussion

To better understand the atomization process in sprays the simulation was carried out with a realistic diesel complex diesel injector geometry. Of interest in this work was to capture the spray evolution from start of injection to near quasi-steady conditions. Prescribing the transient rate-of-injection profile can enable the simulation to capture the transition from low-speed laminar jet flow to turbulent fully atomized spray. The physical conditions for the inflow rate-of-injection generator were based on a selection of peak Reynolds and Weber numbers providing computationally resolvable scales. Scales of interest for wall-resolved turbulent pipe flow is the viscous scale, l_v, estimated as $l_v \sim 5.0\, Re^{-7/8}$; and the Kolmogorov critical radius l_{cr}, (Hinze scale) estimated as $l_{cr} \sim (\sigma^3/\rho^3\epsilon^2)^{1/5}$. Table 2 below illustrates the range of conditions in this work,

Table 2. Fuel specific target conditions studied in transient spray injection event and critical length-scales.

ndodecane	*Re*	*We*	*Oh*	l_v (mm)
P=95bar	6990	54656	0.03	2.1
P=150bar	9204	94737	0.03	1.7
Isooctane	*Re*	*We*	*Oh*	l_v (mm)
P=95bar	19425	72581	0.01	0.88
P=150bar	25573	125806	0.01	0.69

Note that after start of injection, all jets are in a fully atomization regime consistent with $Oh > Oh_{cr.}$.

Start-of-Injection Effects (Isooctane)

The transient mixture formation process of isooctane spray is presented here to examine the effects of start of injection on the spray structure. Figure 4 below shows the evolution the atomizing jet. The formation of azimuthal surface instabilities is indicated by the Rayleigh type behavior at the spray tip as shown in Figure 4(left). The instability growth-rate continues then forming crowns and ligaments that turn into the surrounding drops, Figure 4 (middle-right).

Figure 4. Transient development of isooctane jet (95 bar) showing start-of-injection effects.

Figure 5 shows the behavior of spray at the near nozzle location (*x/D* = 5) at the following time intervals *t* = {0.04, 0.08, 0.12, 0.16} *ms*.

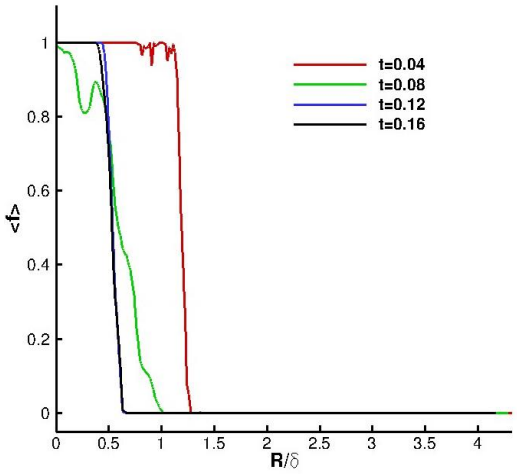

Figure 5. Radial distributions of volume fraction fields showing start-of-injection effects at *x/D* = 5.

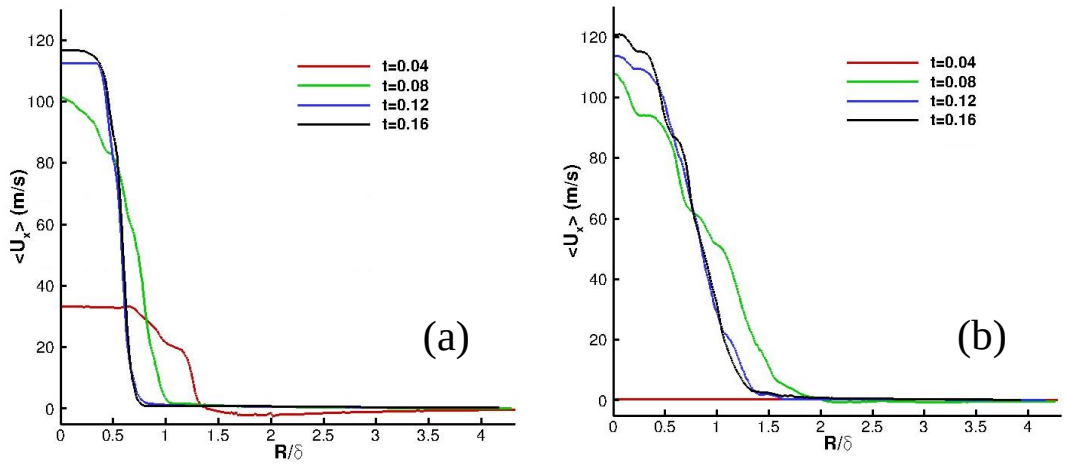

Figure 6. Radial distributions of isooctane mean scalar and velocity fields at 95 bar injection pressure. (a) *x/d* = 5, (b) *x/d* = 10.

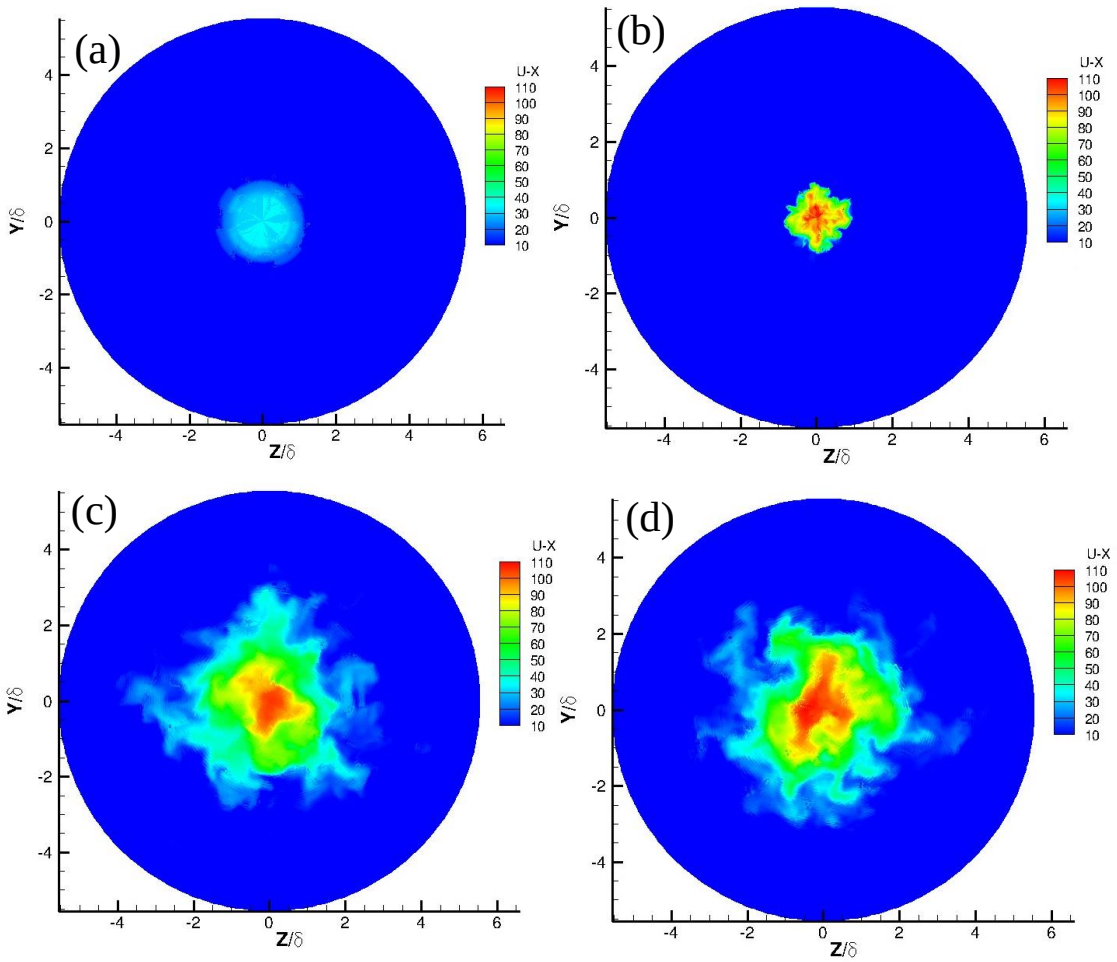

Figure 7. Isooctane instantaneous velocity scalar fields at 95 bar injection pressure at plane location. Axial cut showing flow details at *x/d* =5 at (a) *t =0.04* ms, (b) *t=0.08* ms, (c) *t=0.12* ms, (d) *t=0.16* ms.

The jet width behavior is denoted with the *f* scalar clearly showing radial fluctuations as a result of start-of-injection. At early times, the jet-width captures a FWHM values of ~1.25 R/D decreasing to ~0.6 R/D at later times. This is consistent with experimental observations of transient results [1]. Radial profiles of streamwise velocity at *x/d*=5 (Fig 6a) and *x/d*=10 (Fig 6b) also show the spray start-of-injection behavior. Similarly it shows the decrease in radial signal distribution at later times consistent with Figure 5. Note the simulation captures the linear increase in centerline velocity and jet width at *x/d*=10. To provide more details of the spray structure during start-of-injection Figure 7 presents the cross-sectional contour plots at *x/d*=5 of the instantaneous streamwise velocity fields. The contours shows details of the velocity field and also captures the velocity increase and jet growth behavior in time. These diagnostics are valuable in proving insights into the mixing mechanism of the spray during start-of-injection.

Fuel Effects on Spray Statistics

The simulations were integrated to a common solution time of 100 μs (0.1 ms) for both n-dodecane and isooctane fuels. Note that at this time the spray is close to reaching steady operating conditions with respect to the ROI profiles. Note this also represents a fully open needle valve position. The conditions included two injection pressures, 95 and 150bar, for each fuel as this was specified in Table 2. The velocity and VoF, *f*, scalar fields were averaged in the azimuthal direction to account for dispersion effects, and the results are presented at several downstream axial locations.

Figure 8 compares the fuel specific radial distributions for both of the prescribed injection pressures. Peak velocity values captured compare well with the theoretical Bernoulli nozzle exit velocity (vel ~ 125 m/s, 165 m/s). Figure 8a shows that due to its lower density, isooctane penetrates along the centerline slower than n-dodecane. This effect is strongly pronounced at the spray centerline and decreases radially. Similar behavior is seen on Figure 8b, for higher injection pressure. Also note the simulated jet captures the jet growth at three axial locations marked at 5, 15, 25 diameters downstream of the injector nozzle. For both cases presented Fig 8a and 8b isooctane shows marginally wider jet-width than n-dodecane. Although this was observed, it is concluded that the overall spreading behavior is similar for both conditions at this time interval. However due to the strong transients in this problem longer simulation times are required to ensure that the inflow boundary is in equilibrium. Figure 9 compares the jet mixing behavior through *f* scalar.

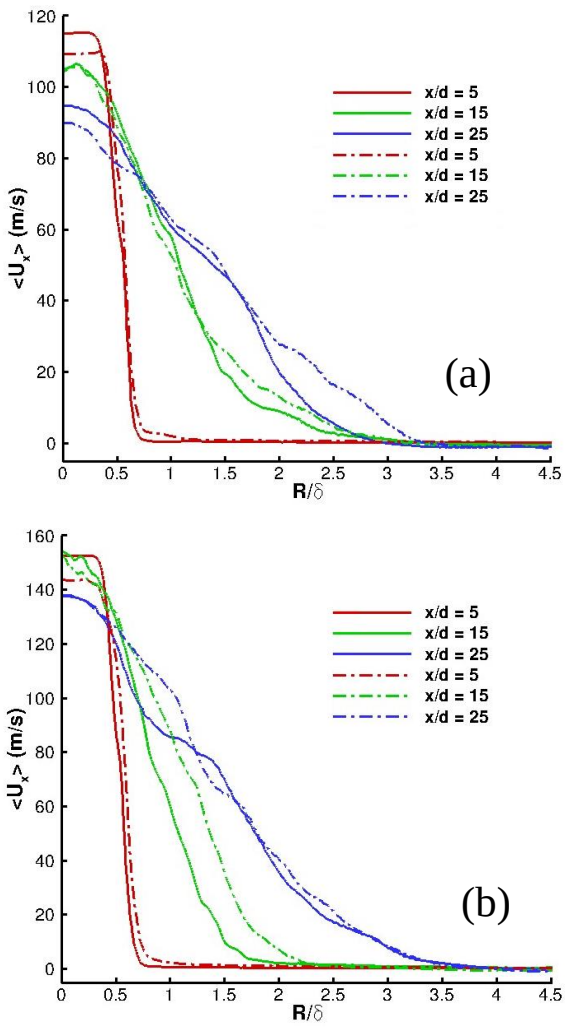

Figure 8. Radial distribution of mean velocity fields at t = 100 μs (0.1 ms) at three axial locations. Solid lines represent dodecane, dashed lines isooctane.(a) 95 bar (b) 150 bar injection pressures.

At 5 diameters downstream the liquid core remains nearly intact at both lower and higher pressures for n-dodecane. This is an indication of a full liquid core region and no disintegration of the spray at this location. Note that isooctane does not retain its intact core at higher pressures. As it is expected, at 15 and 25 diameters both fuels show strong evidence of spray disintegration along the centerline and radially. Note n-dodecane tends to retains more of the liquid structure. The differences between injection pressures are also clear, as the lower pressure spray is able to retain more of its liquid mass, see Figure 9.

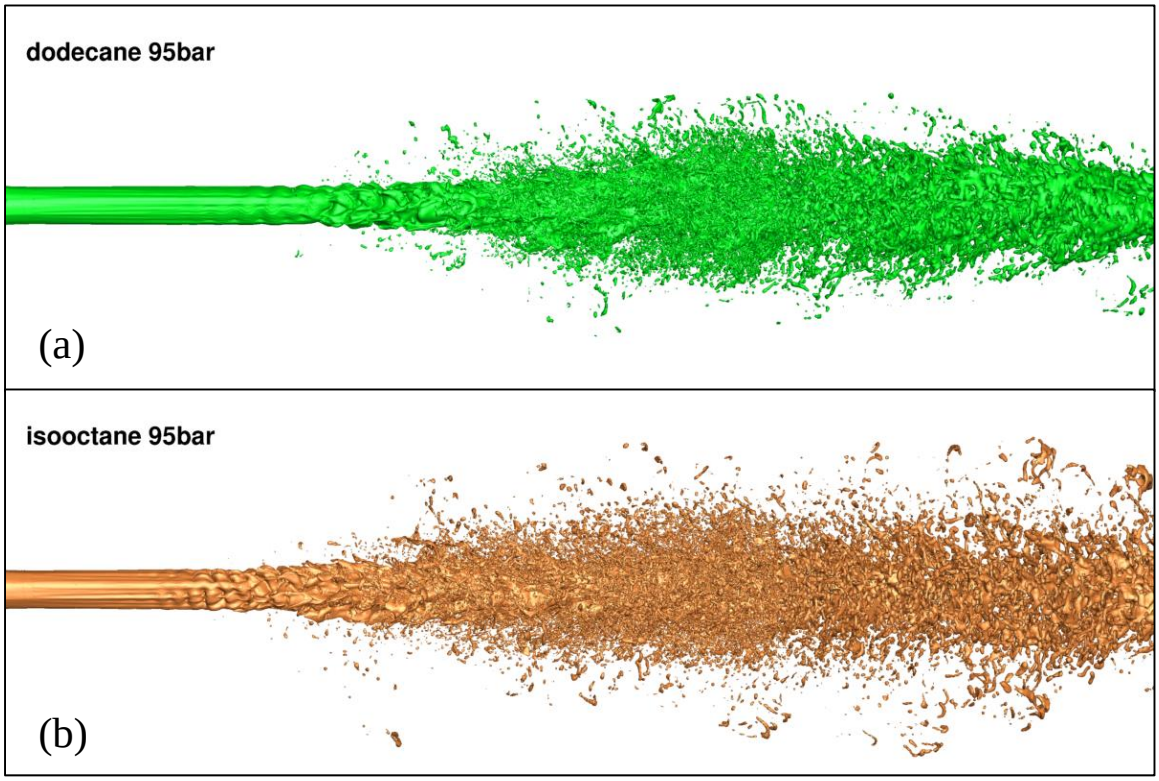

Figure 10. Detailed spray structure at isocontours of f=0.5 at t=100 us for (a) ndodecane and (b) isooctane at injection pressure of 95 bar.

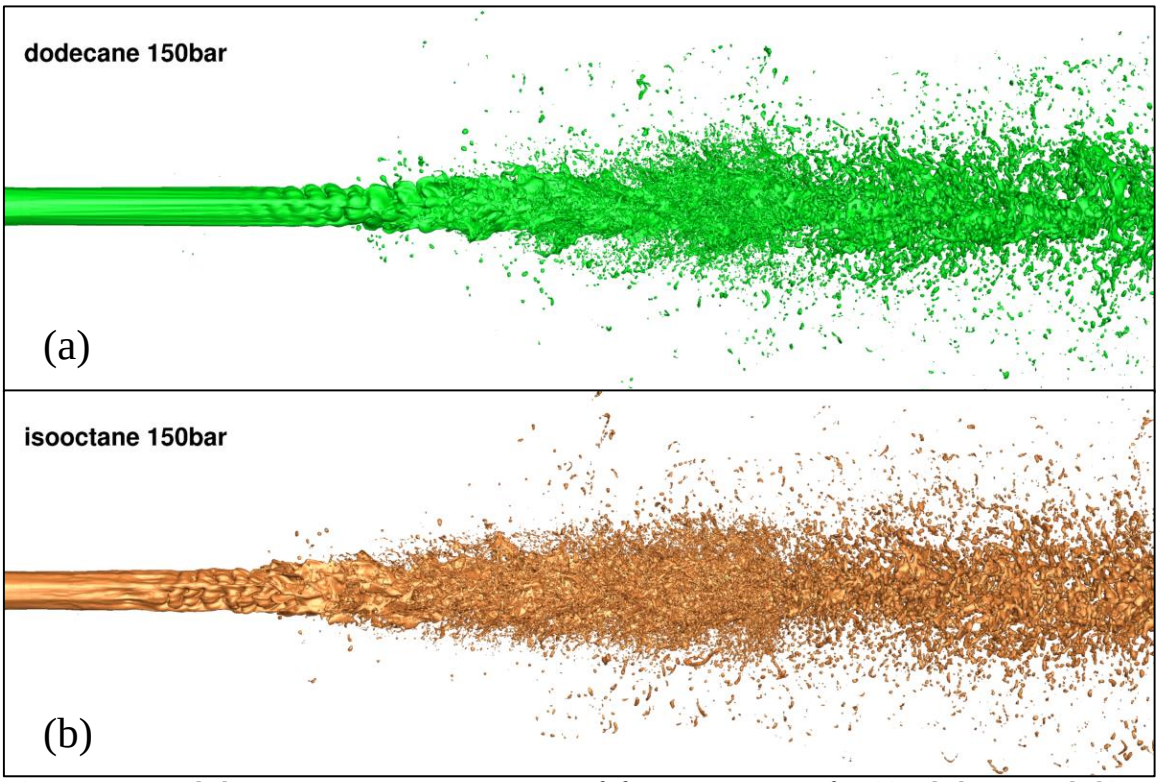

Figure 11. Detailed spray structure at isocontours of f=0.5 at t=100 us for (a) ndodecane and (b) isooctane at injection pressure of 150 bar.

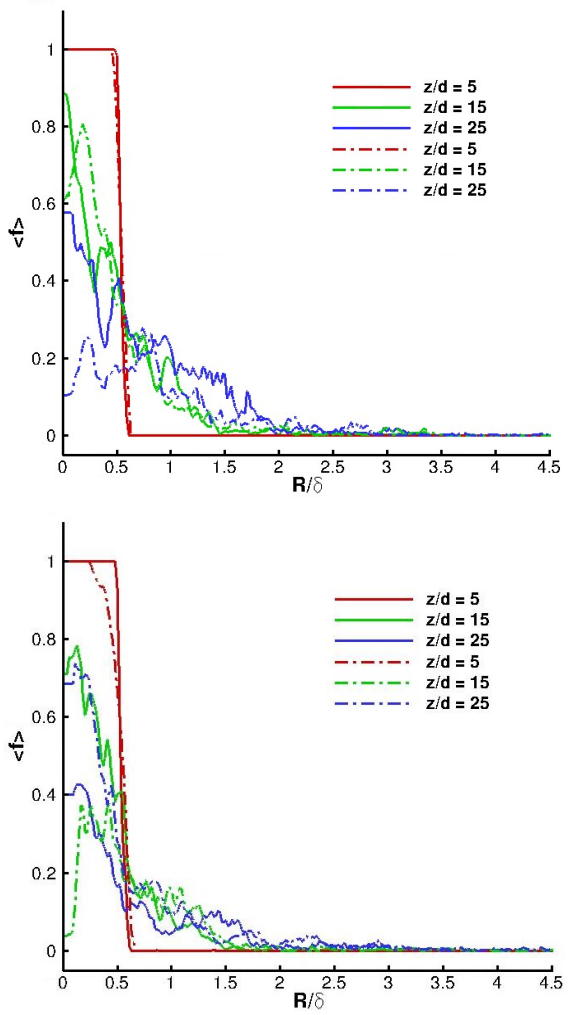

Figure 9. Radial distribution of mean VoF,*f*, fields at t = 100 μs (0.1 ms) at three axial locations. Solid lines represent n-dodecane, dashed lines isooctane

Figure 10-11 shows visualization of the spray surface features through isocontours of VoF f=0.5 scalar, the green and brown color represent n-dodecane and isooctane respectively. The figures show the detailed structure of the atomizing spray showing the upstream azimuthal and radial surface instabilities leading to crown, ligament and a fully atomized spray. Figure 10 compares the spray structure at the lower pressure and shows the impact of the lighter fuel in obtaining a shorter breakup length. This behavior continues at the higher pressure case as seen on Figure 11 which is also consistent with the findings on Figure 9. Comparison with same fuel between the injection pressures also demonstrate shorter breakup lengths. In general, it is seen that the breakup length is controlled by the (i) fuel mass-density, lighter fuels feature shorter lengths, and (ii) injection pressure, higher pressure spray also feature shorter lengths at this working conditions.

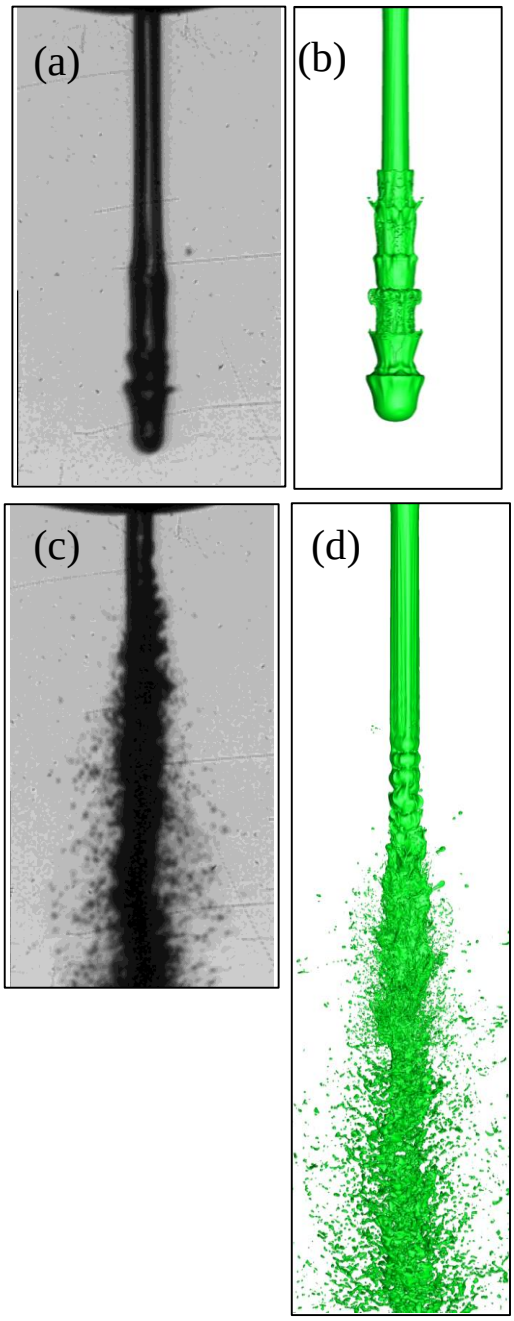

Figure 12. Comparison with high resolution images at P=95bar using n-dodecane fuel. Top row transient spray event at 0.2265 *ms* (a) experiment (b) simulation. Bottom row quasi-steady condition 0.364 *ms* (c) experiment (d) simulation.

Figure 12 presents comparisons with experimental images for n-dodecane fuel at start of injection and quasi-steady condition. The comparison with experiments remain qualitative presently, this is due to

the lack of internal nozzle flow features that are not present in the simulation. This includes sustained pipe flow turbulence, potential cavitation effects and needle fluid-structure interaction. At lower injection pressure (95bar) the simulation shows a breakup length at approximately 8 diameters downstream which is twice as long as the images. Note also that the simulation is sensitive to the inflow conditions, hence variations in the inflow can clearly affect the solution.

Conclusion

In this work, a novel numerical scheme was utilized to simulate primary atomization for diesel sprays using realistic complex injectors. The fuels utilized were n-paraffin (n-dodecane) and iso-paraffin (iso-octane) reference fuels as they are typical constituents for liquid JP8 surrogate fuels. The computational scheme is implemented within a conservative unstructured Cartesian volume of fluids solver that employs state of the art interface transport techniques ideally suited for simulating multiphase flows. The methodology applied was detailed numerical simulation of liquid fueled sprays using bulk inflow conditions from community-wide injector generator module to capture the start-of-injection events and qualitatively compared to experiments. To understand the effect of injection pressure on the fuel's atomization behavior, two conditions were selected obtaining observations about the breakup length, dispersion characteristics, and instantaneous velocity fields. The effects of the bulk condition to capture start-of-injection condition on the multiphase simulation were discussed.

Future works will be targeted at developing models that incorporate more of the nozzle material features, i.e., surface roughness. This will be useful in capturing more realistic flow features and to study the full injection event from start to end of injection across the selected fuels. Numerical diagnostics will be further developed following similar procedures as the experimental imaging to enable direct comparison. In addition, the effect of higher grid resolution on the detailed flow statistics will be pursued.

Acknowledgement

This work was supported in part by high performance computer time and resources from the DoD High Performance Computing Modernization Program (HPCMP) FRONTIER Award. The Army project is titled "Petascale High Fidelity Simulation of Atomization and Spray/Wall Interactions at Diesel Engine Conditions". The simulations were run on the DoD Garnet Cray XE6 computing platform.

The author is also very thankful to Dr. Christopher Powell for characterizing the Army injector geometries at The Advanced Photon Source Facility at Argonne National Laboratory for this work.

References

1. Tess, M.J., Kurman, M., Bravo, L., Kweon, C.B., *27th Annual Conference on Liquid Atomization and Spray Systems*, Raleigh, NC, May 2015.
2. Hirt, C.w., Nichols, B.D., *Journal of Computational Physics*, 39:201–25 (1981).
3. Osher, S., Sethian, J., *Journal of Computational Physics*, 79: 12–49 (1988).
4. Desjardins, O., McCaslin, J., Owkes, M., Brady, P., *Atomization and Sprays*, 23(11):1001-1048 (2013).
5. Li, X., Soteriou, M., *Atomization and Sprays*, 23(11):1049-1078 (2013).
6. Desjardin, O., Pitsch, H., *Atomization and Sprays*, 20(4):311-336 (2010).
7. Desjardin, O., Moureau, V., Pitsch, H., *Journal of Computational Physics*, 227: 8395-8416 (2008).
8. Hermann, M., *Atomization and Sprays*, 21(4): 283-301 (2011).
9. Shinjo, J., Umemura, A., *International Journal of Multiphase Flow*, 36:513-532 (2010).
10. Shinjo, J., Umemura, A., *Proceedings of the Combustion Institute*, 33:2089-2097 (2011).
11. Chenadec, V. L. and Pitsch, H., *Atomization and Sprays*, 23(12): 1139-1165 (2013).
12. Bravo, L., Ivey, C., Kim, D., Bose, S., *Proceedings of Center for Turbulence Research Summer Program*, Stanford, CA 2014.
13. Le Chenadecy, V., Mirjalili, S., Mortazavi, M., Mani, A., *Proceedings of Center for Turbulence Research Summer Program*, Stanford, CA 2014.
14. McCaslin, J., Yeh, C., Desjardin, O., *26th Annual Conference on Liquid Atomization and Spray Systems*, Portland, OR, May 2014.
15. McCaslin, J., Desjardin, O., *Proceedings of Center for Turbulence Research Summer Program*, Stanford, CA 2014.
16. Hermann, M., *Proceedings of Center for Turbulence Research*, Stanford, CA 2014.
17. Kim, D., Mani, A., Moin, P., Stanford Annual Research Briefs, 2013.
18. Kim, D., Ham, F., Herrmann, M., Le, H., *26th Annual Conference on Liquid Atomization and Spray Systems*, Portland, OR, May 2014.
19. Ashgriz, N., Poo, J.Y., *Journal of Computational Physics*, 22: 449-468 (1991).
20. Parker, B.J., Youngs, D.L., *Atomic Weapons Establishment*, 1992.
21. Luning-Prak, D.J., Alexandre, S.M., Cowart, J.S., Trulove, P.C., *Journal of Chemical and Engineering Data*, 59:1334-1346 (2014).
22. Padua, A.A.H., Fareleira, J.M.N.A., Calado, J.C.G., *Journal of Chemical and Engineering Data*, 41:1488-1494 (1996).

1 (PDF)	DEFENSE TECHNICAL INFORMATION CTR DTIC OCA
2 (PDF)	DIRECTOR US ARMY RESEARCH LAB RDRL CIO LL IMAL HRA MAIL & RECORDS MGMT
1 (PDF)	GOVT PRINTING OFC A MALHOTRA
1 (PDF)	DIR USARL RDRL VTP L BRAVO

INTENTIONALLY LEFT BLANK.